



1

2

3 **Development of nascent autotrophic carbon fixation systems in various**
4 **redox conditions of the fluid degassing in early Earth**

5

6 **Sergey A. Marakushev, Ol'ga V. Belonogova**

7 Institute of Problems of Chemical Physics, Russian Academy of Sciences,

8 142432 Chernogolovka, Moscow Region, pr-kt acad. Semionova, 1, Russia

9

10 **Correspondence:** Sergey A. Marakushev (shukaram@yandex.ru; marak@cat.icp.ac.ru)

11

12

13

14 **Abstract.** Strategies for the origin and development of primary metabolism on early Earth
15 were determined by the two main regimes of degassing of Earth in the form of CO₂ or CH₄
16 fluid impulses. Among the existing theories of the autotrophic origin of the life, CO₂ is
17 usually considered the carbon source for nascent autotrophic metabolism. However, the
18 ancestral carbon used in metabolism may have been derived from CH₄ if the outflow of
19 magma fluid to the surface of the Earth consisted mainly of methane. Primary biochemical
20 systems are present in methane degassing regimes developed in an environment of high
21 partial pressure of methane, which is a source of carbon for nascent metabolic systems. Due
22 to the absence of molecular oxygen in the Archaean conditions, this metabolism would have
23 been anaerobic, i.e., oxidation of methane must be realized by inorganic high-potential
24 electron acceptors. In light of the primacy and predominance of CH₄-dependent metabolism
25 in hydrothermal systems of the ancient Earth, we propose a model of carbon fixation, which is
26 a sequence of reactions in a hypothetical methane-fumarate (MF) cycle. Thermodynamics
27 calculations showed a high efficiency of oxidation of methane to acetate (methanotrophic
28 acetogenesis) by oxidized nitrogen compounds in hydrothermal systems. Thermodynamically
29 favorable were also reactions involving the introduction of carbon methane into the
30 intermediates of the proposed MF cycle. The methane oxidation reactions with the use of
31 oxygen of iron mineral buffers are closer to the equilibrium state, which apparently
32 determines the possibilities of primordial cycle flow in the forward or reverse directions.

33



34 **1 Introduction**

35

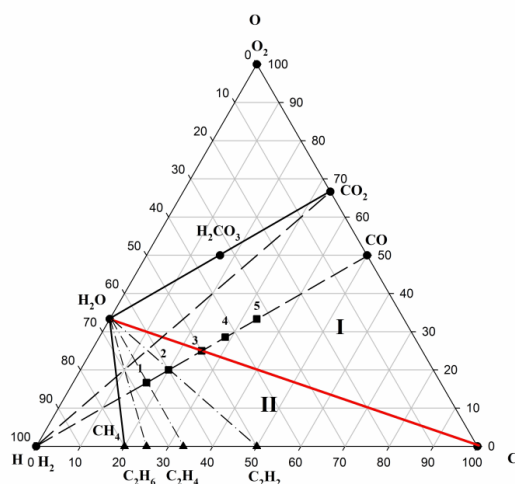
36 The degassing of seismically active planets and satellites manifests in the form of volcanism
37 and fluid flows, allowing us to observe the regime of hydrocarbon degassing of the liquid
38 cores. For example, there is a preponderance of methane on Titan and Enceladus (the
39 satellites of Saturn) (Tobie et al., 2006; Bouquet et al., 2015) and on Europa (the satellite of
40 Jupiter) (Russell et al., 2017). Additionally, high concentrations of methane are assumed to be
41 present on early Mars (Oehler and Etiope, 2017).

42 On Earth, the generation of hydrocarbons from impulse degassing of the Fe-Ni liquid core
43 can be traced since the ancient times. This has been observed in the quartz–methane
44 amygdaline inclusions that occur in the form of relics present even in metamorphic-basaltic
45 rocks of Greenland that are aged at 3.8 billion years (Touret, 2003). Multiple lines of evidence
46 indicate significant concentrations of abiogenic CH₄ in the Archaean atmosphere and
47 hydrosphere (Fiebig et al., 2007; Haqq-Misra et al., 2008; Etiope, 2017; Dodd et al., 2017).
48 Modern volcanism, including hydrothermal emissions at mid-oceanic ridges, is characterized
49 by a primary regime of degassing, with a high carbon dioxide to methane concentration ratio
50 ([CO₂]/[CH₄]) (Reinbow, Von Damm) and also by a secondary regime, with low [CO₂]/[CH₄]
51 (Lost City, Lucky Strike) (Sephton and Hazen, 2013; Konnet et al., 2015). We believe these
52 dominant degassing regimes resulted from various types of magmatism and explosive
53 methane venting tectonics (Marakushev and Marakushev, 2008, 2010; Morner, 2017). There
54 is convincing evidence indicating the presence of at least two main geodynamic regimes of
55 fluid impulse degassing of the hydrogen-rich nickel-iron liquid core in the history of Earth's
56 development (Alldredge, 1984; Milanovsky, 2004; Valet and Herrero-Bervera, 2007; Aubert
57 et al., 2010). These two regimes are believed to have led to the formation of a C–H–O
58 chemical system (Marakushev and Marakushev, 2006, 2010). It is important to note that the
59 core is the most significant reservoir of carbon (Dasgupta and Walker, 2008; Nakajima et al.,
60 2009).

61 Fluids ejected from the liquid core were initially saturated with hydrogen, with oxygenic
62 components being of minor importance. However, when the permeability of silicate shells
63 across the Earth increased (during the expansion of silicate shells of the Earth due to the
64 oscillatory nature of the geomagnetic field), there began a selective migration of hydrogen,
65 the most mobile component, out of the fluid. This process is responsible for hydrogen losing
66 its leading position in ejected fluids and being fundamental to the evolution of low and
67 normal alkalinity magmatism (Marakushev and Marakushev, 2008). In this scenario, the



68 fractionation of chemical components in fluid would result in rich CO₂ solutions (for
 69 example, H₂+2CO = H₂O+0.5CO₂+1.5C and H₂O+CO₂ = H₂CO₃). These solutions are widely
 70 observed in the composition of fluid inclusions in minerals of all igneous rocks of low and
 71 normal alkalinity. In Fig. 1, this region of thermodynamic stability (facies) representing the
 72 paragenetic association of H₂O–C–CO₂ is denoted by (I).



73

74 **Figure 1.** Two regimes of evolution of the C–H–O system on the diagram of its compositions.
 75 Roman numerals denote various regimes of hydrogen fluid evolution: (I) water-carbonic and
 76 (II) water-hydrocarbon solutions, separated by H₂O–C equilibrium (red). Parageneses
 77 (assemblages) of the initial substances (H₂, CO, CO₂) are denoted by dashed sub-lines, while
 78 dash-dotted lines indicate the parageneses (C₂H₆–H₂O, C₂H₄–H₂O, etc) of hydrocarbons
 79 (black triangles) with water. Black squares denote organic substances within the two
 80 component (H₂–CO) system: methanol (1), ethylene glycol (2), acetate (3), succinate (4), and
 81 fumarate (5).

82 The transition to compression of silicate shells prevents hydrogen migration from fluids
 83 and stimulates the production of hydrocarbons within them; for example, consider the
 84 reactions: 3H₂+CO = H₂O+CH₄, 5H₂+2CO = 2H₂O+C₂H₆ (Fig.1, facies II, reducing
 85 conditions). The hydrogen in the reaction like 4H₂+H₂CO₃ = 3H₂O+CH₄ destroys the acid
 86 components in fluids, and this determines the alkaline slope in the development of
 87 magmatism. With increasing alkalinity in the fluid inclusions of igneous minerals invariably
 88 appear different hydrocarbons (Potter and Konnerup-Madsen, 2003; Nivin et al., 2005). This



89 is a two-stage model of the development of the C–H–O system (**I** ↔ **II**), which depends on
90 the composition of Earth's core fluids, and their transformations in magma chambers.

91 The existing theories on the origin of autotrophic life identify carbon dioxide as the
92 unique carbon source for metabolism. This should have occurred at a high partial pressure of
93 CO₂ in the environment (paragenesis CO₂ + H₂O, Fig. 1, facies **I**). However, in geodynamic
94 regime **II**, we demonstrated that the carbon of ancestral metabolism could be hydrocarbonic
95 (paragenesis CH₄+H₂O) if the flow of free energy from the geochemical environment was
96 conjugated to formation reactions of the biomass. Perhaps, these different regimes of fluid
97 degassing determined the emergence and development of various systems of ancient
98 metabolism. In regime **II** (Fig. 1), carbon fixation could occur in the form of methane or other
99 hydrocarbons. For example, in aerobic acetogenesis (CH₄+O₂ = 0,5CH₃COOH+H₂O), more
100 free energy is released in the methane fixation reaction ($\Delta G_{298}^0 = -417.35$ kJ/mol under
101 standard conditions; aqueous constants from (Amend and Shock, 2001)) than in the process of
102 CO₂ fixation (CO₂+2H₂= 0,5CH₃COOH+H₂O; $\Delta G_{298}^0 = -84.75$ kJ/mol).

103 Geochemical evidence strongly indicates highly disparate redox conditions between
104 modern Earth and those in the early Archaean. We consider that the anaerobic geochemical
105 conditions of the Archaean played a decisive role in the origin and development of carbon and
106 energy metabolism, which are vastly different from those observed in the tops of the branches
107 of the modern phylogenetic tree of prokaryotes. Most metabolically-anaerobic
108 chemoautotrophic organisms are either extinct or strongly limited to narrow anoxic ecological
109 niches. Lateral gene transfer and subsequent phylogenetic divergence erased most
110 evolutionary information recorded in ancestral prokaryotic genomes. Currently, it remains
111 unclear which, among the existing genomes, are ancient and sourced from the last universal
112 common ancestor (LUCA) (Martin et al., 2012).

113

114 **2 Anaerobic oxidation of methane**

115

116 The study of anaerobic oxidation of methane (AOM) in modern oxygen-free environments
117 (marine sedimentary rocks, gas-hydrates, mud volcanoes, black smokers, hydrocarbon sipes)
118 has increased in recent years. This direction was sparked by the discovery of anaerobic
119 methanotrophic archaea (Hinrichs et al., 1999) and, subsequently, their structural consortia
120 with sulfate-reducing bacteria (Knittel and Boetius, 2009). A similar relationship was later
121 discovered in archaea species that functions in chemical conjunction with the bacterium
122 *Candidatus Methyloirabilis oxyfera*, which generates nitrite – a terminal electron acceptor



123 in the methane oxidation pathway (Ettwig et al., 2010). Furthermore, the microbiological
124 AOM was recently shown to be directly associated with the reduction of iron and manganese
125 compounds and minerals (Beal, 2009; Ettwig et al., 2016; Oniand Friedrich, 2017; He et al.,
126 2018), as in the reaction $\text{CH}_4 + 8\text{Fe}^{3+} + 2\text{H}_2\text{O} \rightarrow \text{CO}_2 + 8\text{Fe}^{2+} + 8\text{H}^+$ ($\Delta G^{\circ} = -454 \text{ kJ mol}^{-1}$
127 CH_4).

128 Recent studies have suggested that both archaea (ANME-2d) (Haroon et al., 2013) and
129 bacteria (Methylobacter) (Martinez-Cruz et al., 2017), without partners, may themselves be
130 versatile methanotrophs capable of using different oxidants as electron acceptors under
131 different environmental conditions. AOM is proposed to occur by reversal of the canonical
132 methanogenesis pathway. For example, nickel enzyme purified from methanogenic archaea
133 can catalyze the oxidation of methane to methyl coenzyme M ($\text{CH}_4 + \text{CoM-S-S-CoB} \rightarrow$
134 $\text{CH}_3\text{-S-CoM} + \text{HS-CoB}$; $\Delta G^{\circ} = 30 \pm 10 \text{ kJ mol}^{-1}$) (Scheller et al., 2010). Methano- and
135 methylotrophs use different but often interrelated pathways of carbon fixation (Smejkalová et
136 al., 2010). Newly described methanotrophic anaerobic prokaryotes are frequently discovered
137 in various extreme environmental conditions (Semrau et al., 2008), underscoring the
138 functional and phylogenetic diversity of this group. The search for relict forms of anaerobic
139 methanotrophic metabolism continues.

140 In 2013, Wolfgang Nitschke and Michael Russell described the possibility of methane as
141 the sole source of carbon for primordial metabolism (Nitschke and Russell, 2013). They
142 presented a model of the methanotrophic acetogenesis with methane as the carbon source,
143 distinguished by the direction of the reactions from the modern acetyl-CoA pathway. The
144 proposed methane oxidant in this pathway of CH_4 fixation was activated nitric oxide (NO),
145 formed via nitrate/nitrite transformation ('denitrifying methanotrophic acetogenesis') (Russell
146 and Nitschke, 2017). It is assumed that this reverse acetyl-CoA acetogenic pathway was the
147 metabolic foundation for early hydrothermal ecosystems and emergence of LUCA. The
148 authors consider the process of harzburgite (ophiolites) hydrothermal serpentinization in the
149 presence of carbon oxides served as the main source of methane. Nevertheless, Wang et al.
150 (2018) suggest that there is another unified deep high-temperature process (under redox
151 conditions characterizing intrusive rocks derived from sub-ridge melts) of making methane
152 for these hydrothermal areas.

153 The LUCA era apparently proceeded in an environment with high CO_2 partial pressure,
154 whereas the pre-LUCA period proceeded in a reducing environment with a significant
155 predominance of methane. The question thus arises: was this ancestral reverse acetyl-CoA



156 relic pathway the only metabolic CH₄ fixation system, or were there other proto-biochemical
157 mechanisms for the assimilation of carbon?

158 In addition to the acetyl-CoA pathway, autocatalytic CO₂ fixation cycles have been
159 suggested as the first metabolic autocatalytic systems on early Earth (Wächtershäuser, 1990;
160 Smith and Morowitz, 2004; Marakushev and Belonogova, 2009, 2013; Futch, 2011;
161 Braakman and Smith, 2012, 2013). These include a reductive citrate cycle (reverse cycle of
162 tricarboxylic acids, the Arnon cycle), a 3-hydroxypropionate cycle, a 3-hydroxypropionate/4-
163 hydroxybutyrate cycle, a reductive dicarboxylate/4-hydroxybutyrate cycle, and a reducing
164 pentose phosphate (Calvin–Benson–Bassham) cycle. The defined conservative sequences of
165 intermediates of these cycles are modules such that their combination can create a variety of
166 metabolic systems, including the specific pathways of carbon fixation (Lorenz et al., 2011;
167 Marakushev and Belonogova, 2010, 2015; Braakman and Smith, 2012, 2013). To be
168 considered a possible metabolic alternative, assimilating methane through autocatalytic cycle
169 intermediates must satisfy the fundamental requirements of thermodynamics.

170

171 **3 The proposed methane-fumarate (MF) cycle**

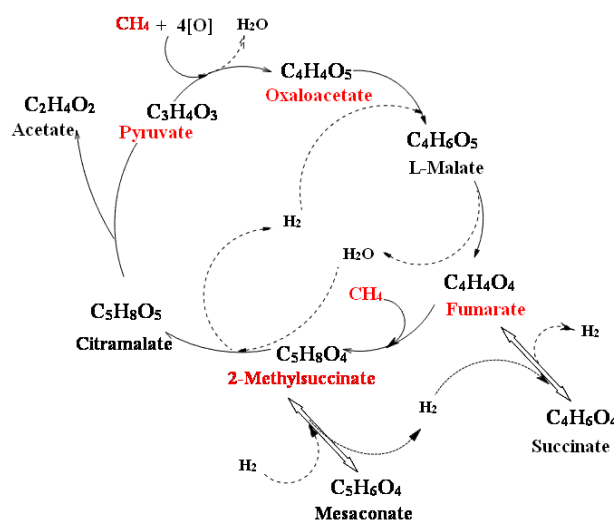
172

173 Based on the hypothesis of primordial anaerobic methanotrophic metabolism origin, we
174 assume that some components and modules of the metabolic cycles ([carboxylic](#) and keto
175 acids, and their parageneses) may also be relicts of ancient methanotrophic acetogenesis. One
176 of the few known reactions of CH₄ fixation is the formation of 2-methylsuccinate as a result
177 of the reaction: fumarate+CH₄ → 2-methylsuccinate (Thauer and Shima, 2008; Austin and
178 Groves, 2011; Haynes and Gonzalez, 2014). Regeneration of fumarate can occur in various
179 metabolic cycles, for example, fumarate+CH₄ → 2-methylsuccinate → mesaconate+2H →
180 citramalate → citramalyl-CoA → pyruvate+acetyl-CoA →→→ oxaloacetate → citrate →
181 isocitrate → 2-oxoglutarate+CO₂+2H → succinyl-CoA+CO₂+2H → succinate →
182 fumarate+2H or fumarate+CH₄ → 2-methylsuccinate → 2-methylsuccinyl-CoA → 2-
183 ethylmalonyl-CoA → butyryl-CoA+CO₂ → crotonyl-CoA+2H → 3-hydroxybutyryl-CoA →
184 4-hydroxybutyryl-CoA → 4-hydroxybutyrate → succinate semialdehyde+2H → succinyl-
185 CoA+2H →succinate → fumarate+2H (Thauer and Shima, 2008). In hydrothermal early-
186 Archaean reducing conditions, the most versatile and widely-used [carboxylic](#) and keto acids
187 could form autocatalytic cycles of methane fixation and release both carbon dioxide and
188 acetate. In the presence of high-potential inorganic oxidants, conditions became possible for
189 the oxidative introduction of methane into the intermediates of putative cycles, seen, for



190 example, in the hypothetical reactions of pyruvate → oxaloacetate and acetate →
 191 oxaloacetate.

192 We propose a simplified model of the methane-fumarate (MF) cycle, Fig. 2, that is
 193 initiated by the reaction of fumarate + methane → 2-methylsuccinate at a high partial pressure
 194 of endogenous methane (facies II, Figure 1), as in Archaean reductive hydrothermal systems (
 195 Dodd et al., 2017). In the hydration and dehydrogenation reactions, 2-methylsuccinate is
 196 converted to citramalate, which is disproportionate to acetate and pyruvate with cleavage of
 197 carbon-carbon bond. The resulting keto acid pyruvate, binding methane, is converted into
 198 keto acid oxaloacetate with the participation of inorganic oxidants (oxidized forms of nitrogen
 199 and transition metals such as iron, manganese, and nickel). Oxaloacetate is transformed into
 200 fumarate in the reactions of the citrate cycle intermediates (Fig. 2). The resulting fumarate
 201 assimilates methane and begins another autocatalytic MF cycle. Without the regeneration of
 202 acetate → pyruvate, the MF cycle would be a synthetic pathway for pyruvate ($C_3H_4O_3$) +
 203 $2CH_4 + 12Fe_2O_3 \rightarrow$ acetate ($C_2H_4O_2$) + pyruvate + $8Fe_3O_4 + 2H_2O$ ($\Delta G_{298}^0 = 11.84$, $\Delta G_{473}^0 =$
 204 -6.49 kJ/mol CH_4), by using pyruvate as a network catalyst. Acetate → pyruvate synthesis
 205 enables positive feedback in the cycle: $5CH_4 + 30Fe_2O_3 + 2$ -methylsuccinate ($C_5H_8O_4$) →
 206 $6H_2O + 20Fe_3O_4 + 2$ -methylsuccinate ($\Delta G_{298}^0 = 14.7$, $\Delta G_{473}^0 = 0.25$ kJ/mol CH_4), or, with
 207 another oxidant, $3CH_4 + 14HNO_2 +$ pyruvate = 2 pyruvate ($C_3H_4O_3$) + $14NO + 11H_2O$ ($\Delta G_{298}^0 = -$
 208 283.3 , $\Delta G_{473}^0 = -347.32$ kJ/mol CH_4), creating network autocatalysis. This model of AOM is
 209 an autocatalytic system of oxidative assimilation of carbon.





211 **Figure 2.** The scheme of the proposed methane-fumarate (MF) cycle. [O], which is the
 212 oxidant of methane, denotes the oxygen of an inorganic redox pair ($\text{HNO}_3/\text{HNO}_2$, HNO_2/NO ,
 213 $\text{H}_2\text{SO}_4/\text{H}_2\text{SO}_3$, $\text{Fe}_2\text{O}_3/\text{Fe}_3\text{O}_4$, etc.). Carbon from methane is introduced into the cycle
 214 components (indicated in red) with the formation of a C–C bond, and the oxygen atoms of the
 215 oxidant are assimilated in the cycle intermediates and in water. The chemical potential of
 216 hydrogen in the environment determines the equilibrium shift in the reactions succinate \leftrightarrow
 217 fumarate and 2-methyl succinate \leftrightarrow mesaconate.

218

219 AOM implies the availability of an oxidant that corresponds to the thermodynamic and
 220 kinetic limitations of this process. In the absence of oxygen, electron acceptors with high
 221 redox potential (such as nitrate, manganese (IV), iron (III), and sulfate) are required.
 222 Thermodynamic calculations of anaerobic methanotrophic acetogenesis reactions in aqueous
 223 hydrothermal conditions that require oxidized compounds such as sulfur, nitrogen, and iron
 224 are considered in Table 1. For example, the free energy of the reaction $\text{CH}_4 + 6\text{Fe}_2\text{O}_3 =$
 225 $0.5\text{CH}_3\text{COOH} + \text{H}_2\text{O} + 4\text{Fe}_3\text{O}_4$ at 473 K is equal to the sum of the free energy of products
 226 formation minus the sum of free energy of the reactants formation at the same temperature
 227 ($\Delta G_{473}^0 = (0.5\Delta G_{\text{CH}_3\text{COOH}}^0 + \Delta G_{\text{H}_2\text{O}}^0 + 4\Delta G_{\text{Fe}_3\text{O}_4}^0) - (\Delta G_{\text{CH}_4}^0 + 6\Delta G_{\text{Fe}_2\text{O}_3}^0) = -6.49$ kJ/mol). It is
 228 obvious that methane oxidation with nitrogen compounds is thermodynamically very
 229 favorable, especially in contrast to the sulfate-sulfite pair.

230

231 **Table 1.** Free Gibbs energy of aqueous reactions (ΔG_{T}^0) of anaerobic methanotrophic
 232 acetogenesis as a function of the oxidant (oxidized forms of nitrogen, sulfur, and iron). The
 233 oxidation of methane to fully ionized and non-ionized forms of acetate is presented at
 234 temperatures of 298 and 473 K at the saturated vapor pressure (P_{SAT}). TR – represents the
 235 temperature regime of the reactions from low (L) to high-temperatures (H). Free energies of
 236 aqueous substances formation at P_{SAT} (Amend and Shock, 2001; Marakushev and
 237 Belonogova, 2012) were used in calculations.

	ΔG_{298}^0 kJ/mol CH_4	ΔG_{473}^0 kJ/mol CH_4	TR
Redox pair of nitrogen			
$\text{CH}_4 + 2\text{NO} = 0.5\text{CH}_3\text{COOH} + \text{H}_2\text{O} + \text{N}_2$	-586.78	-563.18	L
$\text{CH}_4 + 2\text{NO} = 0.5\text{CH}_3\text{COO}^- + 0.5 \text{H}^+ + \text{H}_2\text{O} + \text{N}_2$	-573.39	-538.33	
$\text{CH}_4 + 4\text{NO} = 0.5\text{CH}_3\text{COOH} + \text{H}_2\text{O} + 2\text{N}_2\text{O}$	-582.32	-535.87	L
$\text{CH}_4 + 4\text{NO} = 0.5\text{CH}_3\text{COO}^- + 0.5 \text{H}^+ + \text{H}_2\text{O} + 2\text{N}_2\text{O}$	-568.93	-511.02	
$\text{CH}_4 + 4\text{HNO}_2 = 0.5\text{CH}_3\text{COOH} + 3\text{H}_2\text{O} + 4\text{NO}$	-264.46	-320.79	H
$\text{CH}_4 + 4\text{NO}_2^- + 3.5\text{H}^+ = 0.5\text{CH}_3\text{COO}^- + 4\text{NO} + 3\text{H}_2\text{O}$	-324.71	-398.7	
Redox pair of iron (mineral buffers)			
$\text{CH}_4 + 6\text{Fe}_2\text{O}_3 = 0.5\text{CH}_3\text{COOH} + \text{H}_2\text{O} + 4\text{Fe}_3\text{O}_4$	11.84	-6.49	H
$\text{CH}_4 + 6\text{Fe}_2\text{O}_3 = 0.5\text{CH}_3\text{COO}^- + 0.5 \text{H}^+ + \text{H}_2\text{O} + 4\text{Fe}_3\text{O}_4$	25.23	18.36	



$\text{CH}_4 + 1.5\text{FeS}_2 + 0.5\text{Fe}_3\text{O}_4 = 0.5\text{CH}_3\text{COOH} + \text{H}_2\text{O} + 3\text{FeS}$	44.65	28.85	H
$\text{CH}_4 + 1.5\text{FeS}_2 + 0.5\text{Fe}_3\text{O}_4 = 0.5\text{CH}_3\text{COO}^- + 0.5\text{H}^+ + \text{H}_2\text{O} + 3\text{FeS}$	58.04	53.7	
$\text{CH}_4 + 2\text{Fe}_3\text{O}_4 + 3\text{SiO}_2 = 0.5\text{CH}_3\text{COOH} + \text{H}_2\text{O} + 3\text{Fe}_2\text{SiO}_4$	57.23	16.19	H
$\text{CH}_4 + 2\text{Fe}_3\text{O}_4 + 3\text{SiO}_2 = 0.5\text{CH}_3\text{COO}^- + 0.5\text{H}^+ + \text{H}_2\text{O} + 3\text{Fe}_2\text{SiO}_4$	70.62	41.04	
Sulphate – sulphite redox pair			
$\text{CH}_4 + 2\text{H}_2\text{SO}_4 = 0.5\text{CH}_3\text{COOH} + \text{H}_2\text{O} + 2\text{H}_2\text{SO}_3$	114.88	124.09	L
$\text{CH}_4 + 2\text{SO}_4^{2-} = 0.5\text{CH}_3\text{COO}^- + 0.5\text{H}^+ + \text{H}_2\text{O} + 2\text{SO}_3^{2-}$	128.27	148.94	

238

239 Methanotrophic acetogenesis reactions are energetically more preferable under alkaline
 240 hydrothermal conditions (ionized compound forms). The change in the free energy with
 241 temperature change indicates whether the reaction displays a thermodynamic preference for
 242 low-temperature (L) or high-temperature (H) conditions (Table 1). For example, the sulfate-
 243 oxidase reaction is the most thermodynamically favorable at low-temperature (increasing
 244 ΔG_r^0 with increasing T), whereas the nitrite-oxidase reaction is very favorable at high-
 245 temperature (decreasing ΔG_r^0 with increasing T). Sulfate oxidation is most favorable in its
 246 non-ionized form (acidic conditions) and nitrite oxidation in its ionized form (alkaline
 247 conditions).

248 Table 2 shows the free energy of the carbon fixation reactions by intermediates in the MF
 249 cycle (Fig. 2). The nitrite-nitric oxide ($\text{HNO}_2\text{-NO}$), nitrogen oxide-nitrous oxide ($\text{NO-N}_2\text{O}$),
 250 and nitrogen oxide-molecular nitrogen (NO-N_2) redox pairs were the most thermodynamically
 251 favorable “anaerobic” oxidants. Free energy values calculated at low and high temperatures
 252 (ΔG_{298}^0 and ΔG_{473}^0) informed the estimated temperature regime of these reactions. The redox
 253 nitrogen pairs were clearly the most thermodynamically favorable for methane assimilation
 254 through MF cycle intermediates, but the oxidation reaction with the HNO_2/NO pair is high-
 255 temperature, while that with the $2\text{NO}/\text{N}_2\text{O}$ and $\text{NO}/0.5\text{N}_2$ pairs is low-temperature.

256 The free energy of the CH_4 fixation by MF cycle intermediates strongly favors nitrogen
 257 pairs over mineral buffers pairs, but can be limited by the availability of the oxidant and
 258 kinetically blocked by a large energy barrier. On the other hand reactions with iron mineral
 259 buffers are closer to the equilibrium state, which ultimately determines the possibilities of
 260 primordial cycle flow in the forward or reverse directions (development of methanogenesis or
 261 methanotrophic acetogenesis). An analysis of the oldest known association of microfossils
 262 suggests that methane-cycling methanogen–methanotroph communities were a significant
 263 component of Earth’s early biosphere (Schopf et al., 2017).

264



265 **Table 2.** Free energy of the proposed MF cycle reactions at 298 and 473 K at P_{SAT} with
 266 various oxidants (Fe_2O_3 , Fe_3O_4 , NO, HNO_2) in hydrothermal conditions. For comparison, the
 267 reactions of methane oxidation with molecular oxygen are considered. Free energies of
 268 aqueous substances formation at P_{SAT} (Amend and Shock, 2001; Marakushev and
 269 Belonogova, (El. Suppl. Mat.), 2013) were used in calculations.

Reactions of MF cycle	ΔG^0_{298} kJ/mol	ΔG^0_{473} kJ/mol
$(CH_2)(COOH)_2$ (Fumarate) + $CH_4 = (CH_2)(CH_3CH)(COOH)_2$ (2-Methylsuccinate)	-44.95	-29.97
$(CH_2)(CH_3CH)(COOH)_2 + H_2O = (CH_3CH)CH(OH)(COOH)_2$ (Citramalate) + H_2	96.57	94.14
$(CH_3CH)CH(OH)(COOH)_2 = CH_3COOH$ (Acetate) + $CH_3(CO)COOH$ (Pyruvate)	19.35	1.73
$CH_3(CO)COOH + CH_4 + 2O_2 = CH_2CO(COOH)_2$ (Oxaloacetate) + $2H_2O$	-845.86	-803.44
$CH_3(CO)COOH + CH_4 + 12Fe_2O_3 = CH_2CO(COOH)_2 + 2H_2O + 8Fe_3O_4$	12.52	-17.84
$CH_3(CO)COOH + CH_4 + 3FeS_2 + Fe_3O_4 = CH_2CO(COOH)_2 + 2H_2O + 6FeS$	78.23	52.84
$CH_3(CO)COOH + CH_4 + 4Fe_3O_4 + 6SiO_2 = CH_2CO(COOH)_2 + 2H_2O + 6Fe_2SiO_4$	103.3	27.6
$CH_3(CO)COOH + CH_4 + 8NO = CH_2CO(COOH)_2 + 2H_2O + 4N_2O$	-1175.72	-1076.6
$CH_3(CO)COOH + CH_4 + 8HNO_2 = CH_2CO(COOH)_2 + 6H_2O + 8NO$	-540.08	-646.44
$CH_3(CO)COOH + CH_4 + 4NO = CH_2CO(COOH)_2 + 2H_2O + 2N_2$	-1184.72	-1131.22
$CH_2CO(COOH)_2 + H_2 = CH_2CH(OH)(COOH)_2$ (L-Malate)	-65.49	-55.78
$CH_2CH(OH)(COOH)_2 = (CH_2)_2(COOH)_2 + H_2O$	5.68	-5.26
$(CH_2)_2(COOH)_2 + H_2 = (CH_2)_2(COOH)_2$ (Succinate)	-102.24	-88.88
$(CH_3C=CH)(COOH)_2$ (Mesaconate) + $H_2 = (CH_2)(CH_3CH)(COOH)_2$	-66.53	-54.85

270

271 The reversibility of the reactions in the citrate cycle is mainly determined by the
 272 equilibrium of fumarate+ $H_2 =$ succinate ($\Delta G^0_{298} = -102.24$, $\Delta G^0_{473} = -88.88$ kJ/mol). The
 273 change in the direction of electron flow therein is determined by the chemical potential of
 274 hydrogen (Marakushev and Belonogova, 2009). Therefore, different proto-metabolic cycles
 275 could be formed, for example, the oxidative citrate and reductive 3-hydroxipropionate cycles
 276 (succinate \rightarrow fumarate), the reductive cycle of CO_2 fixation (fumarate \rightarrow succinate), or the
 277 proposed CH_4 fixation cycle (succinate \rightarrow fumarate \rightarrow 2-methylsuccinate). Assimilation of
 278 CH_4 in the MF cycle (pyruvate \rightarrow oxaloacetate, Fig. 2) demonstrates highly favorable
 279 thermodynamics with all redox pairs of nitrogen. The same reaction with hematite (Fe_2O_3)-
 280 magnetite (Fe_3O_4) redox pair is unfavorable at 298 K and becomes favorable at 473 K. Methyl
 281 group formation by the oxidation of methane is limited by kinetics, because the dissociation
 282 energy of the C–H bond in methane (439 kJ/mol) exceeds that of the X–H bond in other
 283 organic molecules, with the exception of the O–H bond in H_2O (497 kJ/mol) and other
 284 oxygen-derived molecular species. Nevertheless, these limitations are overcome in conditions
 285 of high methane and its oxidants concentration and in the presence of metallocatalysts similar



286 to the active center of metalloenzymes, as the key iron-nickel enzyme of methanogenesis,
287 namely, methyl coenzyme M reductase.

288 It is highly possible that the MF cycle existed in a geodynamic regime of high
289 endogenous methane flow in ancient Earth. The thermodynamics of carbon fixation from
290 methane through the archaic MF cycle with its various redox associations of Fe-buffers
291 demonstrate the proximity of these reactions to equilibrium. This proximity enabled multiple
292 possibilities for metabolic reactions to develop in various directions, governed by
293 environmental conditions (temperature, pressure, and chemical potentials of substances). We
294 expect future biochemical studies of AOM to reveal new insights into reaction mechanisms
295 and into energetic and kinetic principles of overall nascent metabolism.

296

297 **4 Anaerobic methane oxidation in a hydrothermal system**

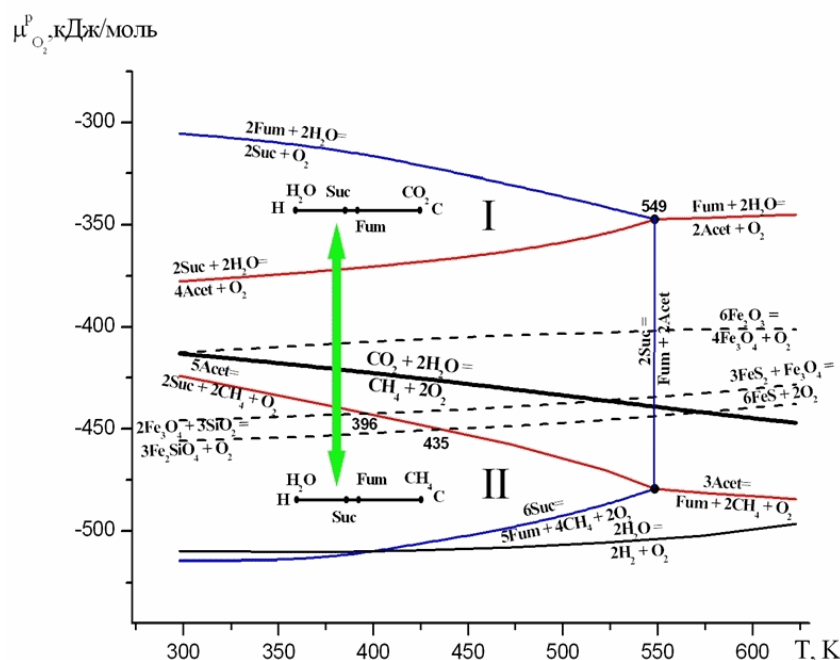
298

299 Under hydrothermal conditions, and in the fluid evolution of the Earth in general (Fig. 1),
300 there is a distinct separation the areas of thermodynamic stability (facies) of CO₂ and CH₄.
301 We represent the hydrothermal system in the form of a phase diagram which displays the
302 chemical potential of oxygen vs. temperature at saturated vapor pressure (P_{SAT}), where
303 temperatures and pressures are below critical thresholds (647,3 K and 22,1 MPa) (Fig. 3). It
304 is a two-component system (extensive parameters: C and H), since oxygen become intensive
305 parameters, as the temperature, and pressure. Oxygen is represented by the chemical potential
306 of O₂ in hydrothermal solution ($\mu_{O_2}^P = RT \ln a_{O_2}$, where a_{O_2} denotes the chemical activity of
307 oxygen). Accordingly, at arbitrary pressure, the nonvariant equilibria in the diagram (points)
308 consist of four phases, and the three-phase equilibria (lines) divide the divariant stability
309 fields (facies) of the two-phase equilibria.

310 The equilibrium CH₄+2O₂ = CO₂+2H₂O (bold line) divides the diagram into the facies of
311 CO₂ (I) and CH₄ (II) and illustrates the two main possibilities for the development of the C–
312 H–O system in the facies carbon dioxide or methane. The CO₂/CH₄ equilibrium determines
313 the oxic and anoxic conditions of the hydrothermal system. Intermediates of the MF cycle are
314 acetate, succinate, and fumarate, and we considered their metastable equilibria and
315 parageneses. In all phase space under consideration, there are fumarate facies. The
316 equilibrium of 5Fum+4CH₄+2O₂ = 6Suc at low-temperature (Fig. 3), is located in the region
317 of very low partial pressures of oxygen, whereas the equilibrium of Fum+2CH₄+O₂ = 3Acet
318 at high-temperature occurs in facies of high pressures. Acetate and succinate facies (contoured
319 with a red and blue lines, respectively) completely encompass the equilibrium of CH₄+O₂ =



320 $\text{CO}_2 + \text{H}_2\text{O}$. That is, in hydrothermal solution, the parageneses of some components within the
 321 MF cycle are stable in both the CO_2 and the CH_4 facies. The whole system can develop in
 322 either of two directions as the chemical potential of oxygen changes: 1. the formation of low-
 323 temperature (Suc- H_2O) and high-temperature (Fum- H_2O) paragenesis in CO_2 facies (I) and 2.
 324 the formation of low-temperature (Suc- CH_4) and high-temperature (Fum- CH_4) paragenesis in
 325 CH_4 facies (II). Thus, within these facies, protobiochemical systems supporting carbon
 326 fixation in the form of CO_2 or CH_4 can develop, and methane facies (II) represent a broad area
 327 of CH_4 assimilation by carboxylic acids and keto acids in an aqueous environment. The high
 328 stability of the succinate-fumarate-acetate paragenesis in hydrothermal systems at 200°C
 329 (473 K) was experimentally shown (Estrada et al., 2017).



330

331 **Figure 3.** Diagram of the chemical potential of oxygen ($\mu^{\text{P}}_{\text{O}_2}$) - temperature (T, K) at
 332 saturated vapor pressure (P_{SAT}). The areas of thermodynamic stability of substances and their
 333 parageneses were calculated according to the method described in Marakushev & Belonogova
 334 [2009]. Points (indicated by temperature values) and lines represent four-phase and three-
 335 phase equilibria, separating the two-phase divariant fields of substance stabilities. The bold
 336 line represents the equilibrium of $\text{CO}_2 \leftrightarrow \text{CH}_4$ and separates their areas of thermodynamic
 337 stability (I and II). The dashed lines are equilibria of mineral buffers: hematite-magnetite,
 338 $\text{Fe}_2\text{O}_3/\text{Fe}_3\text{O}_4$ (HM), pyrite-pyrrhotite-magnetite, $\text{FeS}_2 + \text{Fe}_3\text{O}_4/\text{FeS}$ (PPM), and quartz-



339 magnetite-fayalite, $\text{SiO}_2+\text{Fe}_3\text{O}_4/\text{Fe}_2\text{SiO}_4$ (QMF). We provide linear diagrams of the two-
340 component C–H system in the CO_2 and CH_4 facies. The transition between the facies when
341 the chemical potential of oxygen changes is indicated by a green arrow. Abbreviation:
342 Succinate – Suc, Fumarate – Fum, Acetate –Acet.

343

344 Mineral buffers up to 549 K are located in the facies of succinate, but the equilibrium of
345 HM remains in the area of thermodynamic CO_2 stability (facies I). PPM and QMF equilibria
346 occur in methane facies II and intersect the fundamental equilibrium of $2\text{Suc}+2\text{CH}_4+\text{O}_2 =$
347 5Acet , the clear basis of methanotrophic acetogenesis. Magnetite (Fe_3O_4) facies (between HM
348 and QMF equilibria) encompass CH_4/CO_2 equilibrium in nearly the entire temperature range
349 of the hydrothermal system under consideration, and hematite (Fe_2O_3) becomes an effective
350 methane oxidant over the entire temperature range. This determines the P/T conditions for the
351 development of methanotrophic systems with the participation of hematite as an oxidant, e.g.
352 reaction pyruvate ($\text{C}_3\text{H}_4\text{O}_3$)+ $\text{CH}_4+12\text{Fe}_2\text{O}_3 =$ oxaloacetate ($\text{C}_4\text{H}_4\text{O}_5$)+ $2\text{H}_2\text{O}+8\text{Fe}_3\text{O}_4$ is
353 favorable at high temperature, Table 2. The formation of magnetite also occurs above 396 K
354 for the PPM buffer and above 435 K for the QMF buffer. Thus, the redox conditions of
355 magnetite stability correspond to the formation conditions of CH_4 assimilating systems. The
356 presence of magnetite in the early Archaean ocean was shown by (Li et al., 2017]. The
357 functional importance of the keto group for chemical transformation of the C–C bond was
358 experimentally demonstrated under hydrothermal conditions by Yang et al., (2018), where
359 magnetite and hematite minerals catalyzed the C–C and C–H fragmentation of ketones.

360 Prior to the great oxidative event of 2.2-2.4 billion years ago on the Earth's surface, the
361 oxidation potential of the hematite-magnetite redox buffer apparently determined the
362 chemical potential of environmental oxygen. Shibuya et al. (2016) demonstrated the necessity
363 of iron compound redox reactions for the process of relict methanogenesis and
364 methanotrophic acetogenesis to function, as in the most ancient forms of metabolism.

365

366 5 Conclusion

367

368 In general, cyclic planetary fluid flows drive Earth's chemical evolution, leading to the
369 formation of geobiochemical systems of carbon fixation. Impulses of CO_2 and CH_4 degassing
370 on our planet must have contributed to the development of various types of carbon
371 metabolism. It is generally accepted that autotrophic metabolism is the fixation (assimilation)
372 of inorganic carbon solely in the form of CO_2 , but CH_4 is also deep and inorganic; therefore,



373 carbon fixation from methane is also a manifestation of autotrophic metabolism. The variety
374 of modern autotrophic carbon fixation seems to be due to the association of the different
375 metabolic modules created by a diverse assemblage of ancestral metabolic modules presented
376 in the LUCA. Lateral gene transfer and subsequent phylogenetic divergence erased much of
377 the evolutionary information in the genomes; thus, it is not clear which genes among the
378 sequenced genomes are truly ancient (i.e., traced to LUCA) (Martin et al., 2016). When a CO₂
379 degassing regime began to dominate on our planet, relict systems of methanotrophy were
380 forced to die out or to be thrown back into uncommon and extreme ecological niches. If we
381 consider LUCA as a relatively recent player in the evolution of life (Cornish-Bowden and
382 Cárdenas, 2017), then the number of carbon-fixing metabolic systems in putative pre-LUCA
383 organisms should be incommensurably greater than the present numbers.

384 In the process of development of CO₂ fixation systems on Earth, the main problem was
385 the presence of electron donors (therefore, evolution created selective reducing agents:
386 NADH, NADPH, FADH), whereas the fixation of CH₄ essentially depended on the presence
387 of electron acceptors. In the hydrothermal systems, oxygen-containing nitrogen compounds
388 are the best oxidants, but we believe that the redox pairs of hematite-magnetite and quartz-
389 magnetite-fayalite create a specific area of chemical potential of oxygen that satisfies the
390 thermodynamic requirements of oxidation and assimilation of methane by protometabolic
391 pathways. Hydrothermal systems of ancient Earth may have been very similar to those that
392 currently exist on some extraterrestrial cosmic bodies, such as Europa or Enceladus. The
393 degassing of these cosmic bodies can currently support methane metabolism, but the problem
394 is to know if there are electron acceptors there (Russell et al., 2017).

395

396 **Author Disclosure Statement**

397 No competing financial interests exist.

398

399 **References**

400

401 Allredge, L.R.: A discussion of impulses and jerks in the geomagnetic field, *J. Geophys.*

402 *Res.*, 89, 4403–4412, doi: 10.1029/JB089iB06p04403, 1984.

403 Amend, J.P., and Shock, E.L.: Energetics of overall metabolic reactions of thermophilic and

404 hyperthermophilic Archaea and Bacteria, *FEMS Microbiol. Rev.*, 25, 175–243, doi:

405 10.1016/S0168-6445(00)00062-0, 2001.



- 406 Aubert, J., Tarduno, J.A., and Johnson, C.L.: Observations and models of the long-term
407 evolution of earth's magnetic field, *Space Sci. Rev.*, 155, 337–370, doi:
408 10.1007/s11214-010-9684-5, 2010.
- 409 Austin, R.N., and Groves, J.T.: Alkane-oxidizing metallo enzymes in the carbon cycle,
410 *Metallomics*, 3, 775–787, doi: 10.1039/c1mt00048a, 2011.
- 411 Beal, E.J., House, C.H., and Orphan, V.J.: Manganese - and iron-dependent marine methane
412 oxidation, *Science*, 325, 184–187, doi: 10.1126/science.1169984, 2009.
- 413 Bouquet, A., Mousis, O., Waite, J.H., and Picaud, S.: Possible evidence for a methane source
414 in Enceladus' ocean, *Geophys. Res. Lett.*, 42, 1334–1339, doi: 10.1002/2014GL063013,
415 2015.
- 416 Braakman, R., and Smith, E.: The emergence and early evolution of biological carbon-
417 fixation, *PLOS Comput. Biol.*, 8, 1–16, doi: 10.1371/journal.pcbi.1002455, 2012.
- 418 Braakman, R., and Smith, E.: The compositional and evolutionary logic of metabolism, *Phys.*
419 *Biol.*, 10, 1–63, doi: 10.1088/1478-3975/10/1/011001, 2013.
- 420 Cornish-Bowden, A., and Cárdenas, M.L.: “Life Before LUCA,” *J. Theor. Biol.*, 434, 68–74,
421 doi: 10.1016/j.jtbi.2017.05.023, 2017.
- 422 Dasgupta, R., and Walker, D.: Carbon solubility in core melts in a shallow magma ocean
423 environment and distribution of carbon between the Earth's core and the mantle,
424 *Geochim. Cosmochim. Acta*, 72, 4627–4641, doi: 10.1016/j.gca.2008.06.023, 2008.
- 425 Dodd, M.S., Papineau, D., Grenne, T., Slack, J.F., Rittner, M., Pirajno, F., O'Neil, J., and
426 Little, C.T.S.: Evidence for early life in Earth's oldest hydrothermal vent precipitates,
427 *Nature*, 543, 60–64, doi: 10.1038/nature21377, 2017.
- 428 Estrada, C.F., Mamajanov, I., Hao, J., Sverjensky, D.A., Cody, G.D., and Hazen, R.M.:
429 Aspartate transformation at 200 °C with brucite [Mg(OH)₂], NH₃, and H₂: implications
430 for prebiotic molecules in hydrothermal systems, *Chem. Geol.*, 457, 162–172, doi:
431 10.1016/j.chemgeo.2017.03.025, 2017.
- 432 Etiope G.: Abiotic methane in continental serpentinization sites: an overview. *J.: Proced.*
433 *Earth Planet. Sci.*, 17, 9–12, doi: 10.1016/j.proeps.2016.12.006, 2017.
- 434 Ettwig, K.F., Butler, M.K., Le Paslier, D., Pelletier, E., Mangenot, S., Kuypers, M.M.,
435 Schreiber, F., Dutilh, B.E., Zedelius, J., de Beer, D., Gloerich, J., Wessels HJ, van Alen
436 T, Luesken F, Wu ML, van de Pas-Schoonen KT, Op den Camp HJ, Janssen-Megens,
437 E.M., Francoijs, K.J., Stunnenberg, H., Weissenbach, J., Jetten, M.S., and Strous, M.:
438 Nitrite-driven anaerobic methane oxidation by oxygenic bacteria, *Nature*, 464, 543–548,
439 doi: 10.1038/nature08883, 2010.



- 440 Ettwig, K.F., Zhu, B., Speth, D., Keltjens, J.T., Jetten, M.S.M., and Kartal, B.: Archaea
441 catalyze iron-dependent anaerobic oxidation of methane, *Proc. Natl. Acad. Sci.*, 113,
442 12792–12796, doi: 10.1073/pnas.1609534113, 2016.
- 443 Fiebig, J., Woodland, A.B., Spangenberg, J., and Oschmann, W.: Natural evidence for rapid
444 abiogenic hydrothermal generation of CH₄. *Geochim. Cosmochim. Acta*, 71, 3028–
445 3039, doi: 10.1130/G25598A.1, 2007.
- 446 Fuchs, G.: Alternative pathways of carbon dioxide fixation: Insights into the early evolution
447 of life? *Ann. Rev. Microbiol.*, 65, 631–658, doi: 10.1146/annurev-micro-090110-
448 102801, 2011.
- 449 Haqq-Misra, J., Domagal-Goldman, S.D., Kasting, P.J., and Kasting, J.F.: A revised, hazy
450 methane greenhouse for the Archaean Earth, *Astrobiol.*, 8, 1127–1137, doi:
451 10.1089/ast.2007.0197, 2008.
- 452 Haroon, M.F., Hu, S., Shi, Y., Imelfort, M., Keller, J., Hugenholtz, P., Yuan, Z., and Tyson,
453 G.W.: Anaerobic oxidation of methane coupled to nitrate reduction in a novel archaeal
454 lineage, *Nature*, 500, 567–570. DOI: 10.1038/nature12375, 2013.
- 455 Haynes, C.A., and Gonzalez, R.: Rethinking biological activation of methane and conversion
456 to liquid fuels, *Nature Chem. Biol.*, 10, 331–339, doi: 10.1038/nchembio.1509, 2014.
- 457 He, Z., Zhang, Q., Feng, Y., Luo, H., Pan, X., and Gadd, G.M.: Microbiological and
458 environmental significance of metal-dependent anaerobic oxidation of methane,
459 *Sci. Total Environ.*, 610–611, 759–768, doi: 10.1016/j.scitotenv.2017.08.140,
460 2018.
- 461 Hinrichs, K.U., Hayes, J.M., Sylva, S.P., Brewer, P.G., and DeLong, E.F.: Methane-
462 consuming archaeobacteria in marine sediments, *Nature*, 398, 802–805. doi
463 :10.1016/S0146-6380(00)00106-6, 1999.
- 464 Knittel, K., and Boetius, A.: Anaerobic oxidation of methane: progress with an unknown
465 process. *Ann. Rev. Microbiol.*, 63, 311–334, doi:
466 10.1146/annurev.micro.61.080706.093130, 2009.
- 467 Konn, C., Charlou, J.L., Holm, N.G., and Mousis, O.: The production of methane, hydrogen,
468 and organic compounds in ultramafic-hosted hydrothermal vents of the Mid-Atlantic
469 Ridge, *Astrobiol.*, 15, 381–399, doi: 10.1089/ast.2014.1198, 2015.
- 470 Li, Yi-L., Konhauser, K.O. and Zhai, M.: The formation of magnetite in the early Archean
471 oceans, *Earth Planet. Sci. Lett.*, 466, 103–114, doi: 10.1016/j.epsl.2017.03.013, 2017.
- 472 Lorenz, D.M., Jeng, A., and Deem, M.W.: The emergence of modularity in biological
473 systems, *Phys. Life Rev.*, 8, 129–160, doi: 10.1016/j.plprev.2011.02.003, 2011.



- 474 Marakushev, A.A., and Marakushev, S.A.: PT facies of elementary, hydrocarbon, and organic
475 substances, *Dokl. Earth Sci.*, 406, 141–147, doi: 10.1134/S1028334X0601034X, 2006.
- 476 Marakushev, A.A., and Marakushev, S.A.: Formation of oil and gas fields, *Lithol. Miner.*
477 *Resour.*, 43, 454–469, doi: 10.1134/S0024490208050039, 2008.
- 478 Marakushev, A.A., and Marakushev, S.A.: Fluid evolution of the Earth and origin of the
479 biosphere, in: *Man and the Geosphere*, edited by: Florinsky, I.V., Nova Science
480 Publishers Inc, New York, 3–31, 2010.
- 481 Marakushev, S.A., and Belonogova, O.V.: The parageneses thermodynamic analysis of
482 chemoautotrophic CO₂ fixation archaic cycle components, their stability and self-
483 organization in hydrothermal systems, *J. Theor. Biol.*, 257, 588–597, doi:
484 10.1016/j.jtbi.2008.11.032, 2009.
- 485 Marakushev, S.A., and Belonogova, O.V.: Metabolic design and biomimetic catalysis of the
486 archaic chemoautotrophic CO₂ fixation cycle, *Mos. Univer. Chem. Bull.*, 65, 212–218,
487 doi: 10.3103/S0027131410030211, 2010.
- 488 Marakushev, S.A., and Belonogova, O.V.: Thermodynamic factors of natural selection in
489 autocatalytic chemical systems, *Dokl. Biochem. Biophys.*, 444, 131–136, doi:
490 10.1134/S1607672912030015, 2012.
- 491 Marakushev, S.A., and Belonogova, O.V.: The divergence and natural selection of
492 autocatalytic primordial metabolic systems, *Orig. Life Evol. Biosph.*, 43, 263–281, doi:
493 10.1007/s11084-013-9340-7, 2013.
- 494 Marakushev, S.A., and Belonogova, O.V.: The Chemical Potentials of Hydrothermal Systems
495 and the Formation of Coupled Modular Metabolic Pathways, *Biophysics*, 60, 542–552,
496 doi: 10.1134/S0006350915040168, 2015.
- 497 Martin, R.S., Ilyinskaya, E., and Oppenheimer, C.: The enigma of reactive nitrogen in
498 volcanic emissions, *Geochim. Cosmochim. Acta*, 95, 93–105, doi:
499 10.1016/j.gca.2012.07.027, 2012.
- 500 Martin, W.F., Weiss, M.C., Neukirchen, S., Nelson-Sathi, S., and Sousa, F.L.: Physiology,
501 phylogeny, and LUCA, *Microbial Cell*, 3, 582–587, doi: 10.15698/mic2016.12.545,
502 2016.
- 503 Martinez-Cruz, K., Leewis, M.-C., Herriott, I.C., Sepulveda-Jauregui, A., Anthony, K.W.,
504 Thalasso, F., and Leigh, M.B.: Anaerobic oxidation of methane by aerobic
505 methanotrophs in sub-Arctic lake sediments, *Sci. Total Environ.*, 607–608, 23–31, doi:
506 10.1016/j.scitotenv.2017.06.187, 2017.



- 507 Milanovsky, E.E.: Geopolity in the evolution of the Earth, in: The planet Earth. Encyclopedic
508 reference. Tectonics and geodynamics, edited by: Krasnyi, L.I., Petrov, O.V., and
509 Blueman, B.L., VSEGEI, SPb, Russia, 41–55, 2004.
- 510 Morner, N-A.: Methane hydrate in crystalline bedrock and explosive methane venting
511 tectonics, *Earth-Sci. Rev.*, 169, 202–212, doi: 10.4236/ojer.2017.62005, 2017.
- 512 Nakajima, Y, Takahashi, E, Suzuki, T., and Funakoshi, K.I.: ‘Carbon in the core’ revisited,
513 *Phys. Earth Planet. Interiors*, 174, 202–211, doi: 10.1016/j.pepi.2008.05.014, 2009.
- 514 Nitschke, W., and Russell, M.J.: Beating the acetyl-CoA pathway to the origin of life, *Phil.*
515 *Trans. Royal Soc. London, Series B*, 368, 20120258, doi: 10.1098/rstb.2012.0258,
516 2013.
- 517 Nivin, V.A., Treloar, P.J., Konopleva, N.G., and Ikorsky, S.V.: A review of the occurrence,
518 form and origin of C-bearing species in the Khibiny alkaline igneous complex, Kola
519 Peninsula, NW Russia, *Lithos*, 85, 93–112, doi: 10.1016/j.lithos.2005.03.021, 2005.
- 520 Oehler, D.Z., and Etiope, G.: Methane seepage on Mars: where to look and why, *Astrobiol.*,
521 17, 1233–1264, doi: 10.1089/ast.2017.1657, 2017.
- 522 Oni, O.E. and Friedrich, M.W.: Metal oxide reduction linked to anaerobic methane oxidation,
523 *Trends Microbiol.*, 25, 88–90, doi: 10.1016/j.tim.2016.12.001, 2017.
- 524 Potter, J., and Konnerup-Madsen, J.: A review of the occurrence and origin of abiogenic
525 hydrocarbons in igneous rocks, in: *Hydrocarbons in Crystalline Rocks*, edited by:
526 Petford, N., and McCaffrey, K.J.W., Special Publications, 214, Geological Society,
527 London, 151–173, doi:10.1144/GSL.SP.2003.214.01.10, 2003.
- 528 Russell, M.J., Murray, A.E., and Kevin, P.H.: The possible emergence of life and
529 differentiation of a shallow biosphere on irradiated icy worlds: The example of Europa,
530 *Astrobiol.*, 17, 1265–1273, doi: 10.1089/ast.2016.1600, 2017.
- 531 Russell, M.J., and Nitschke, W.: Methane: Fuel or Exhaust at the Emergence of Life?
532 *Astrobiol.*, 17, 1053–1066, doi: 10.1089/ast.2016.1599, 2017.
- 533 Schopf, J.W., Kitajima, K., Spicuzza M.J., Kudryavtsev A.B., and Valley, J.W.: SIMS
534 analyses of the oldest known assemblage of microfossils document their taxon-
535 correlated carbon isotope compositions, *Proc. Natl. Acad. Sci. USA*, 115, 53–58, doi:
536 10.1073/pnas.1718063115, 2017.
- 537 Scheller, S., Goenrich, M., Boecher, R., Thauer, R.K., and Jaun, B.: The key nickel enzyme
538 of methanogenesis catalyses the anaerobic oxidation of methane, *Nature*, 465, 606–
539 609, doi: 10.1038/nature09015, 2010.



- 540 Semrau, J.D., DiSpirito, A.A., and Murrell, J.C.: Life in the extreme: thermoacidophilic
541 methanotrophy, *Trends Microbiol.*, 16, 190–193, doi: 10.1016/j.tim.2008.02.004, 2008.
- 542 Sephton, M.A., and Hazen, R.M.: On the origins of deep hydrocarbons, reviews in
543 mineralogy, *Rev. Miner. Geochem.*, 75, 449–465, doi: 10.2138/rmg.2013.75.14, 2013.
- 544 Shibuya, T., Russell, M.J., and Takai, K.: Free energy distribution and hydrothermal mineral
545 precipitation in Hadean submarine alkaline vent systems: Importance of iron redox
546 reactions under anoxic conditions, *Geochim. Cosmochim. Acta*, 175, 1–19, doi:
547 10.1016/j.gca.2015.11.021, 2016.
- 548 Smejkalová, H., Erb, T.J., and Fuchs, G.: Methanol assimilation in *Methylobacterium*
549 *extorquens* AM1: demonstration of all enzymes and their regulation, *PLoS ONE*, 5,
550 e13001, doi: 10.1371/journal.pone.0013001, 2010.
- 551 Smith, E. and Morowitz, H.G.: Universality in intermediary metabolism, *Proc. Natl. Acad.*
552 *Sci. USA*, 101, 13168–13173, doi: 10.1073/pnas.0404922101, 2004.
- 553 Thauer, R.K., and Shima, S.: Methane as fuel for anaerobic microorganisms, *Ann. NY Acad.*
554 *Sci.*, 1125, 158–170, doi: 10.1196/annals.1419.000.90, 2008.
- 555 Tobie, G., Lunine, J.I., and Sotin, C.: Episodic outgassing as the origin of atmospheric
556 methane on Titan, *Nature*, 440, 61–64, doi: 10.1038/nature04497, 2006.
- 557 Touret, J.L.R.: Remnants of early Archaean hydrothermal methane and brines in pillow-
558 breccia from the Isua-Greenstone Belt, West Greenland, *Precambrian Res.*, 126, 219–
559 233, doi: 10.1016/S0301-9268(03)00096-2, 2003.
- 560 Valet, J.-P., and Herrero-Bervera E.: Geomagnetic reversals, in: *Encyclopedia of Earth*
561 *Sciences Series*, edited by: Gubbins, D., and Herrero-Bervera, E., Springer, Dordrecht,
562 the Netherlands, 339–346, 2007.
- 563 Yang, Z., Gould, I.R., Williams, L.B., Hartnett, H.E., and Shock, E.L.: Effects of iron-
564 containing minerals on hydrothermal reactions of ketones, *Geochim. Cosmochim. Acta*,
565 223, 107–126, doi: 10.1016/j.gca.2017.11.020, 2018.
- 566 Wächtershäuser, G.: Evolution of the first metabolic cycles, *Proc. Natl. Acad. Sci. USA*, 87,
567 200–204, doi: 10.1073/pnas.87.1.200, 1990.
- 568 Wang, D.T., Reeves, E.P., McDermott, J.M., Seewald, J.S., and Ono, S.: Clumped
569 isotopologue constraints on the origin of methane at seafloor hot springs, *Geochim*
570 *Cosmochim Acta* 223, 141–158, doi: 10.1016/j.gca.2017.11.030, 2018.